

# Fabrication, Characterization and Optimization of Multiphasic Zein/Cartilage-derived Matrix/CP/Gelatin Composite Scaffolds for Potential Bone Tissue Engineering Applications

Azadeh Shahroodi<sup>1</sup>, Sogol Hooshyar<sup>2</sup>, Davood Yari<sup>3</sup>, Jebraeil Movaffagh<sup>4</sup> and Ali Moradi<sup>5,6\*</sup>

<sup>1</sup>Department of Mechanical and Industrial Engineering, Atlantic Technology University, MET Gateway, Galway, Ireland

<sup>2</sup>Department of Biomedical Engineering, Islamic Azad University Mashhad Branch, Mashhad, Iran

<sup>3</sup>Cellular and Molecular Biology Research Center, Health Research Institute, Babol University of Medical Sciences, Babol, Iran

<sup>4</sup>Pharmacological Research Center of Medicinal Plants, Mashhad University of Medical Sciences, Mashhad, Iran

<sup>5</sup>Orthopedic Research Center, Mashhad University of Medical Sciences, Mashhad, Iran

<sup>6</sup>Clinical Research Development Unit, Ghaem Hospital, Ahmabad Street, Mashhad, Iran

## Abstract

**Introduction:** Creating an ideal scaffold for bone tissue engineering requires specific characteristics. Composite materials, combining the advantages of polymers and ceramics, offer tailored properties and enhanced functionality. This study aimed to fabricate, characterize and optimize multi-phasic composite scaffolds with spiral backbones for potential bone tissue engineering applications.

**Methods:** Composite scaffolds were fabricated via electrospinning using 24.5% Zein and varying concentrations of Calcium Phosphate (CP) (15%, 20% and 25%). Ribbon-shaped electrospun Zein/CP composite mats were structured into spiral forms, placed in cylindrical Teflon molds, filled with a blended slurry (Zein/cartilage-derived matrix/CP/gelatin), snap-frozen and lyophilized to form multi-phasic composite scaffolds. Mechanical, FESEM and FTIR analyses assessed compressive strength, architectural properties (porosity, pore size and interconnectivity), thermogravimetric behaviour, chemical functional groups and biocompatibility.

**Results and Discussion:** The study evaluated composite scaffolds for bone tissue engineering, focusing on varying CP concentrations in Zein nanofibers. The scaffold with a 20% CP concentration exhibited Young's modulus of approximately 3.26 MPa. FESEM analysis revealed highly interconnected pores for scaffolds with 15% CP, with a pore size of  $50.12 \pm 6.07$  and a porosity of 69.72%. FTIR and DSC analyses confirmed scaffold robustness. Comparisons with bone tissue showed similarities in compressive strength but slight differences in porosity. Despite this, the scaffold demonstrated potential for further optimization. Overall, the scaffold with 20% CP exhibited superior mechanical strength, with larger pore sizes indicating better potential for cell growth and nutrition, high-lighting its promise for bone tissue engineering applications.

**Keywords:** Zein • Electrospinning • Nanofiber • Scaffold • Bone tissue engineering • Mechanical properties

## Introduction

In cutting-edge regenerative medicine, bone tissue engineering offers hope for improving how we treat bone defects and injuries compared to traditional methods. Scientists aim to create a similar environment to the natural bone by using compatible scaffolds with cells and signalling factors. This helps in regenerating strong, weight-bearing tissues. There's been a lot of focus on developing composite materials for orthopedic purposes that can handle heavy loads. However, despite progress, a big challenge remains: scaffold materials often aren't strong enough, making it hard to engineer bone tissue effectively. The strength of a scaffold is crucial for mimicking the structure of natural bone and enduring everyday pressures [1]. Strong mechanical properties are needed to give the right support, stability and

function, allowing the scaffold to help with regeneration. But many scaffold materials available today don't meet these needs, which is a problem for bone tissue engineers [2]. Constructs meant for Bone Tissue Engineering (BTE) should have a large surface area, good porosity to allow cells to move, compatibility with living tissue, strong mechanical properties similar to natural bone, the ability to prevent microbial growth to avoid bone infections and gradual breakdown to encourage new bone tissue formation. Scaffold materials must possess sufficient stiffness, resilience and load-bearing capacity to withstand mechanical pressures and facilitate proper bone formation, ensuring the long-term stability of the regenerated tissue without compromise [3]. Artificial polymeric materials offer excellent flexibility in design, impressive mechanical properties, compatibility with living tissues and the ability to degrade gradually [4]. Composite scaffolds have been extensively explored for their suitability in bone tissue engineering due to their ability to mimic the complex structure and composition of natural bone [5]. These scaffolds are composed of polymers and ceramics with different mechanical properties and degradation rates. Achieving a balance between compatibility with living tissues, biological activity and mechanical strength is crucial in scaffold design. While compatibility and biological activity address cellular response and integration, mechanical strength is essential for providing adequate support during the healing and remodelling phases [6]. However, controlling material distribution and alignment within composite scaffolds can pose challenges, affecting their overall structural integrity. Furthermore, selecting appropriate materials for composite scaffolds is critical in achieving the desired mechanical, biological and degradation properties. Zein, the main protein stored in

\*Address for Correspondence: Ali Moradi, Clinical Research Development Unit, Ghaem Hospital, Ahmabad Street, Mashhad, Iran; Tel: +989155074614; Email: ralimoradi@gmail.com

**Copyright:** © 2024 Shahroodi A, et al. This is an open-access article distributed under the terms of the Creative Commons Attribution License, which permits unrestricted use, distribution and reproduction in any medium, provided the original author and source are credited.

**Received:** 10 April, 2024, Manuscript No. jtse-24-132020; **Editor Assigned:** 12 April, 2024, PreQC No. P-132020; **Reviewed:** 19 April, 2024, QC No. Q-132020; **Revised:** 19 April, 2024, Manuscript No. R-132020; **Published:** 26 April, 2024, DOI: 10.37421/2157-7552.2024.15.351

corn, makes up around (45-50% of the corn's protein content [7]. Due to its abundance of nonpolar amino acids such as leucine, proline and alanine, zein stands out as one of the most hydrophobic proteins [7]. Additionally, it exhibits thermal stability [8] and resistance to oxygen penetration, making it a valuable material. Alongside its biodegradability and compatibility with living organisms, zein is highly elastic and can form films, making it suitable for various applications such as coatings, fibers, biodegradable films, controlled release systems and plastics [9]. Research has explored how zein can enhance the stability and availability of various gallic acids, including carotene, ferulic acid, curcumin, (-)-epigallocatechin gallate (EGCG) and tannin [10]. Aytac Z, et al. used electrospinning to encapsulate a combination of natural antimicrobials, such as thymol oil, citric acid and nisin, within zein fibers [11]. In another study, Ansarifard E and Moradinezhad F incorporated thyme essential oil into zein fibers using electrospinning, with acetic acid as the solvent [12]. Electrospinning is a unique and adaptable technique that employs electrostatic forces to produce fragile fibers, ranging from a few nanometers to several micrometers in diameter [13]. Introduced by Anton and Formhals, this method has since been used to spin a wide range of polymer solutions successfully and melts into thin fibers for various industrial applications, including filtration, textile manufacturing, electronics, sensors, catalysis and medicine [14]. In the field of biomedicine, electrospun fibers, particularly nanofibers crafted from biocompatible and biodegradable polymers, are widely used in wound dressing [15,16], tissue engineering, medical implants [17] and drug delivery systems [13]. Despite the apparent simplicity of the electrospinning process, achieving fibers with optimal properties requires careful adjustment of several variables. These variables encompass process parameters such as voltage, flow rate and the distance between the spinneret and collector, as well as solution characteristics like concentration, surface tension, viscosity and electrical conductivity and environmental conditions such as temperature and humidity [18]. Consequently, the traditional method of optimization can be both time-consuming and costly and it may not always lead to the identification of the optimal conditions among these variables. Decellularization treatments are crucial for xenogeneic scaffolds, as they help remove residual DNA, alpha-Gal epitopes, or human leukocyte antigens that could trigger an immune response [19]. Essentially, cartilage decellularization involves using detergents to break down chondrocytes in the lacunae, followed by washing to remove debris and genetic material [20]. This process involves a combination of physical, chemical and enzymatic steps. However, decellularizing cartilage is challenging due to its dense structure. Various methods have been proposed to improve detergent diffusion into the tissue, such as finely fragmenting the sample. Yet, while finer processing enhances detergent penetration, it can compromise the unique multiphase architecture of articular cartilage. Alternatively, decellularization without tissue homogenization preserves cartilage architecture while reducing immunological and xenogeneic concerns. However, achieving the optimal blend and ratio of materials for composite scaffolds can be daunting, requiring extensive examination and optimization of various components. Composite scaffolds typically degrade over time, promoting new bone formation. Yet, the degradation rate of each constituent may vary, leading to uneven breakdown within the scaffold, compromising its mechanical integrity during the healing process. The long-term biocompatibility of composite scaffolds is still under investigation, as some materials may produce harmful by-products during degradation, hindering bone regeneration and triggering inflammation or immune reactions. Scaling up composite scaffold fabrication from small-scale laboratory production to large-scale manufacturing poses significant challenges, including ensuring consistent quality, reproducibility and cost-effectiveness when dealing with complex composite structures. Ongoing research aims to overcome these limitations to enhance the practical application of composite scaffolds for bone tissue engineering. However, the scaffold's structure significantly influences mechanical properties, cell infiltration, adhesion, growth and blood vessel formation. This study aimed to create a multiphase composite scaffold comprising a helical backbone of electrospun Zein/calcium phosphate (CP) combined with a porous composite of cartilage-derived matrix (CDM)/CP/gelatin through freeze-drying for bone tissue engineering applications.

## Materials and Methods

### Materials

The following materials were procured in analytical grade and utilized without additional purification: Zein (Sigma-Aldrich, Spain) and Glacial acetic acid (>99.7%, Dr. Mojallali, Iran). Hydroxyapatite and tricalcium phosphate were synthesized by Osveh company (OsvehOss-Synthetic Bone Graft). Calf hooves were sourced from a local abattoir with the requisite authorization from the General Department of Veterinary Medicine. The methodology outlined in our prior publication was adhered to for the extraction of articular cartilage [20].

### Methods

**Scaffold fabricatio:** The scaffold fabrication process is illustrated in Figure 1. In steps one and two, Zein/CP membranes were fabricated using the electrospinning technique. The various manufacturing parameters for nanofiber production are detailed in Table 1. Subsequently, in step 4, the membranes were cut into strips, spiral-rolled and inserted into a Teflon mold. The mold was then filled with slurry composed of CDM/CP/gelatin, snap-frozen and subsequently freeze-dried to produce the final cylindrical scaffolds.

**Analysis of solution characteristics:** To investigate the impact of incorporating different concentrations of CP into zein solution, viscosity and conductivity measurements were performed on all solutions before the electrospinning process. Viscosity analysis was conducted using a Brookfield R/S+ Rheometer rotational rheometer equipped with the CC25 spindle, covering shear rates ranging from 5 to 200 s<sup>-1</sup>. Electrical conductivity was evaluated using an RS232 Conductivity Meter 8301.

**Composite slurry:** Calf hooves were procured from a local abattoir with the necessary permission granted by the General Department of Veterinary Medicine. The method outlined in our previous study was adhered to for the extraction of articular cartilage [21]. Subsequently, the cartilage fragments were finely minced using a scalpel within a glass petri dish containing cold phenylmethylsulfonyl fluoride (PMSF) and then homogenized to produce slurry. This slurry underwent decellularization as per a previously established protocol. The resulting cartilage-derived matrix (CDM) underwent centrifugation and the supernatant was discarded [22]. A composite blend was formulated using 15% (wt%) CDM, calcium phosphate at concentrations of 15%, 20% and 25% (wt%) and 5% (wt%) gelatin. The calcium phosphate consisted of 30% hydroxyapatite (HA) and 70% tricalcium phosphate (TCP). Ultra-pure water (UPW) served as the solvent for the formation of the composite slurry [23].

**Field Emission Scanning Electron Microscopy (SEM):** The surface characteristics of zein-CP nanofibers and pill-shaped multi-phasic Zein/CP/CDM/gelatin composite scaffolds were assessed using Field Emission Scanning Electron Microscopy (FESEM) (MIRA3, TESCAN CO., Czech) with an accelerating voltage of 20 kV. Before imaging, the samples underwent sputter coating with gold-palladium for 300 seconds at 25 mA. The average fiber diameter was determined by measuring 50 randomly selected fibers using image analysis software.

**Tensile test:** The electrospun Zein/CP mats were precisely cut into strips measuring 60 × 10 mm with a thickness of 0.1 mm. These strips were then firmly attached to a rectangular frame to ensure precise positioning on the universal tester machine. Equipped with a 6 N capacity load cell, the universal tester conducted tensile testing at a crosshead speed of 2 mm/min, with a minimum of five replicates for each sample type. The elastic modulus was determined by analyzing the slope of the linear portion of the stress-strain curves. Data analysis was performed using a T-test, with statistical significance set at P<0.05.

**Compressive strength test:** The compressive strength of the multiphase cylindrical Zein/CP/CDM/Gelatin composite scaffolds was assessed using the aforementioned universal testing machine, equipped with a 100 N capacity load cell, at a cross-head speed of 2 mm/min. The elastic modulus was calculated using the method previously described. Additionally, a fatigue test was performed using the same universal testing machine, at a cross-head speed of 0.5 mm/min, with 20 loading cycles.

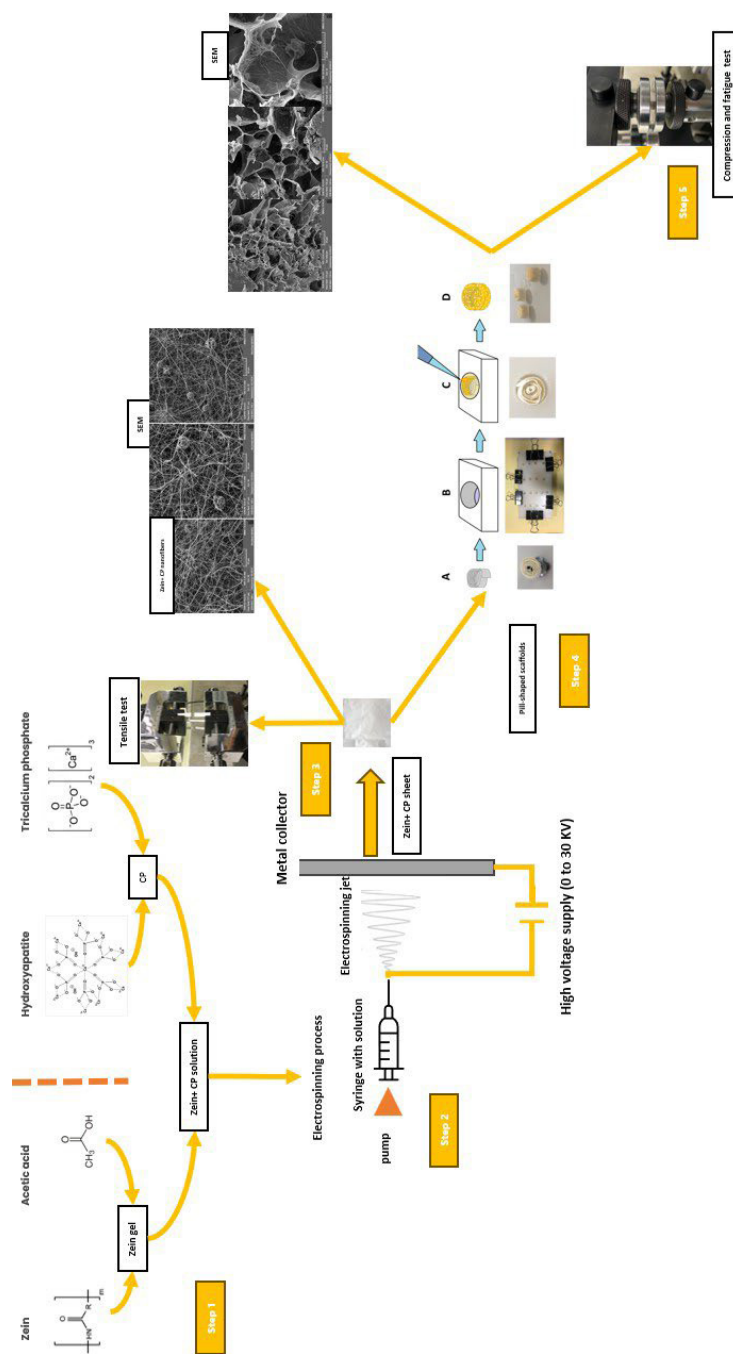


Figure 1. The protocol of manufacturing Zein/CP/CDM/Gelatin scaffold.

Table 1. Polymer concentrations.

Polymer (%)	Acetic Acid (%)	CP (%)	CDM (%)	Gelatin (%)
24.50	99.90	15	15	5
24.50	99.90	20	15	5
24.50	99.90	25	15	5

**Porosity and pore size measurement:** The porosity of the composite scaffolds was measured and calculated using a previously described computer assisted micro-volumetric method [24]. Utilizing scanning electron microscope (SEM) images, ImageJ software was employed to quantify the porosity and size of the pores within the decorative Zein/Cp/CDM/Gelatin composite scaffolds.

**Fourier Transform Infrared (FTIR) analysis:** The FTIR spectra of Nano fibrous mats were obtained using an FTIR spectrophotometer at room temperature. The wavelength range covered 4000-450  $\text{cm}^{-1}$ , with an accumulation of 64 scans and a resolution of 4 $\text{cm}^{-1}$ .

## Results

In this study, zain nanofibers with different concentrations of CP (TCP+HA) were successfully synthesized using the electrospinning technique, using carefully selected parameters including solvent selection, final concentration of polymer and CP and flow rate. After the characteristics of zein nanofibers were determined, gelatin and CDM were added to the folded nanofibers and subsequently, the mechanical properties of the resulting scaffolds were evaluated.



**Morphological study of zein nanofiber**

The viscosity test conducted on zein solution and zein solution with varying CP concentrations revealed a significant increase in viscosity from zein to zein+CP solution ( $P < 0.01$ ). This difference was also significant between CP 15% and CP 20%, but no significant difference was observed between CP 20% and CP 25% ( $P > 0.5$ ). In Figure 2 depicts the FESEM micrographs of zein NFs containing different volumes of CP. The outcomes of viscosity measurements and SEM analyses are presented in Table 2. The findings indicate a notable elevation in viscosity and NFs diameter ( $P < 0.05$  and  $P < 0.001$ , respectively) between zein NFs and zein+15% CP. This difference was significant between zein+15% CP and zein+20% CP, but there was no significant difference between zein+20% CP and zein+25% CP Figure 2. The nanofiber diameters are also uneven. A significant difference in fiber diameter was observed between Zein24.5%-CP15% and Zein24.5%-CP25%. In Figure 2, Ceramic (CP) Particles and the corresponding EDX peaks are also depicted at 500x magnification of different nanomats along with the EDX spectrum (Table 2).

**Tensile strength of electrospun zein/cp composite nanofibrous mats**

The Young’s moduli of electrospun Zein/CP composite nanofibrous mats at three different CP concentrations are presented in (Figure 3). With the incorporation of the CP component into the Zein nanofibers, a significant decrease in the mechanical properties of the fibers was observed. An increase in CP concentration increased fiber resistance among the CP concentration groups. Specifically, nanofibers containing 25% CP exhibited the highest Young’s modulus (0.58 MPa) among all CP concentration groups (Figures 2-4).

**Micromorphology of multiphasic zein/cdm/cp composite scaffolds**

The next step involved the formation of a bone scaffold of nanofibers with a CP component. Following the procedure outlined in Figure 1, step 4, Zein+CP nanofibers were immersed in CDM and gelatin to increase their mechanical properties. As shown in Figure 4, the cross-sectional FESEM coronal

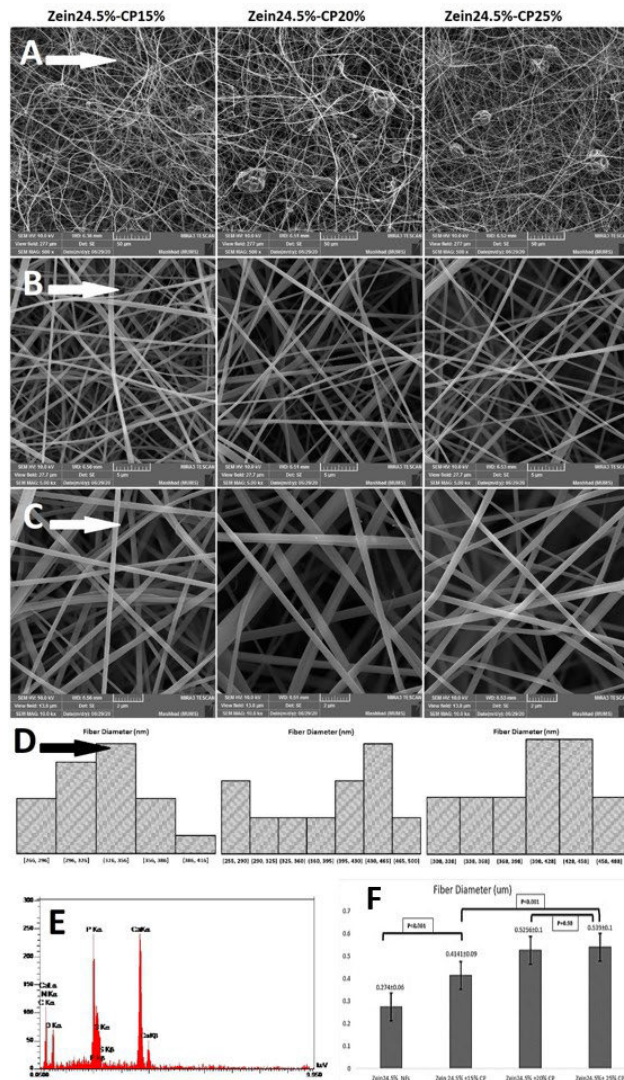


**Figure 2.** FESEM images of electrospun Zein-CP mats at 15%, 20% and 25% CP concentrations at three various magnifications: **A)** 500X: showing the random alignment of the fibers as well as the distribution of CP particles, **B)** 5000X and **C)** 10000X: showing the uneven fiber diameters and alignment, **D)** Histograms of fiber diameter distribution, **E)** Energy dispersive X-ray (EDX) analysis of electrospun Zein-CP mat and **F)** Comparison (T-test) of fiber diameters in electrospun Zein-CP mats at 15%, 20% and 25% CP concentrations.

**Table 2.** Viscosity and diameter measurements.

	Zein	Zein+CP (15%)	Zein+CP (20%)	Zein+CP (25%)
<b>Viscosity (Pa.s)</b>	0.55 ± 0.03	0.755 ± 0.01	-	-
<b>Diameter (µm)</b>	0.274 ± 0.06	0.414 ± 0.09	0.526 ± 0.1	0.540 ± 0.1

micro- morphology of Zein/CP/CDM/gelatin multiphase cylindrical composite scaffolds shows the lamellar and porous surface of the scaffold along with the pore size and interconnectivity. It is worth noting that Zein/CP20%/CDM/gelatin composite scaffolds showed a significant pore size compared to the other two types of composite scaffolds with CP concentrations of 15% and 25%, as shown in (Figure 4).

**Porosity:** Based on ImageJ analysis, no significant difference in porosity was observed in CDM/CP/gelatin scaffolds with 15%, 20% and 25% CP concentrations. However, the porosity of CDM/CP/gelatin scaffolds was higher than that of Zein/CP/CDM/gelatin multiphase composites. As shown in (Figure 5), Zein/CP-15%/CDM/gelatin composites had higher porosity compared to Zein/CP20%/- CDM/gelatin composites (P=0.21) and Zein/CP25%/CDM/gelatin (P=0.04) showed.

**Compressive strength of multiphasic Zein/CDM/CP composite scaffolds**

Figure 6B shows the stress/strain curves for Zein/CDM/CP/gelatin multiphase composite scaffolds with three different CP concentrations (15%,

20% and 25%). In addition, (Figure 6) shows Young’s modulus of the Zein/CDM/CP/gelatin multiphase composite scaffolds compared to the porous CDM/CP/gelatin scaffolds with 15%, 20% and 25% CP concentrations. Based on Figure 6, it is clear that the incorporation of an electrospun Zein/CP helical backbone has significantly increased the compressive strength of the CDM/CP/gelatin porous scaffold.

**FTIR test**

Due to the proteinaceous nature of both Zein and collagen in CDM, similar and overlapping bands are observed in the FTIR spectrum. Specifically, the carbonyl stretch of the amide group at 1650 cm<sup>-1</sup> corresponds to peptide groups (amide I). The amide II band at 1540cm<sup>-1</sup> is associated with the vibration of N-H band deformations, while the band at 1230 cm<sup>-1</sup> corresponds to the vibration of C-N band deformations. Additionally, the C=O stretching vibrations are represented by the peak at 1720 cm<sup>-1</sup> in collagen. Furthermore, the N-H and O-H stretching bands of amino acids in the range of 3500-2800 cm<sup>-1</sup> are characteristic of Zein (Figure 7).

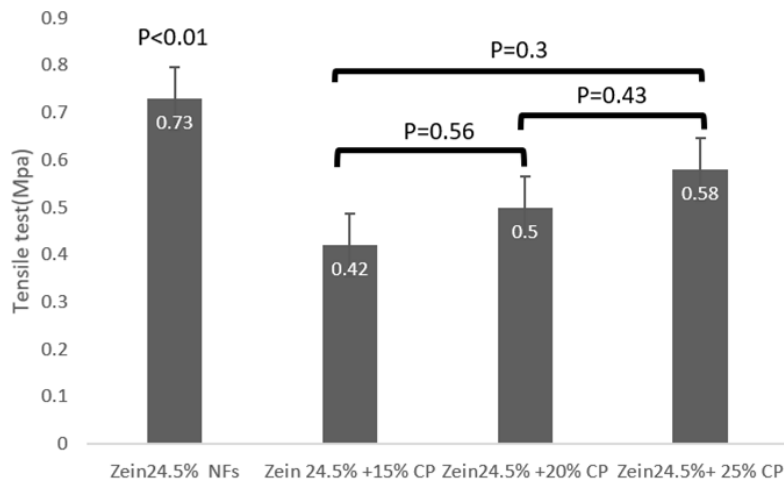


Figure 3. The Young’s moduli of electrospun Zein and Zein/CP composite nanofibrous mats with 15%, 20% and 25% CP concentrations.

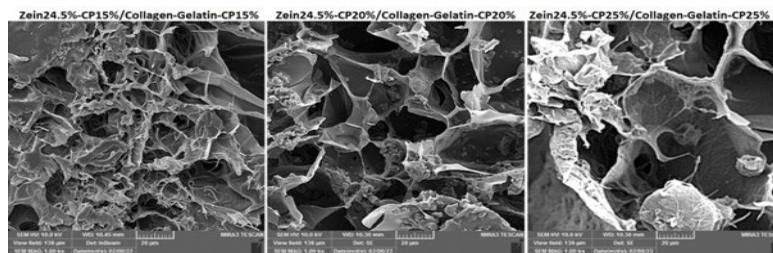


Figure 4. FESEM cross-sectional micrographs of the multiphasic Zein/CDM/CP composite scaffolds with three different CP concentrations (15%, 20% and 25%) at four different magnifications (100X: layered structure of the spiral backbone, 1000X: overall pore shapes and diameters, 2000X: surface morphology of the pores and 5000X: tangled web of fibers).

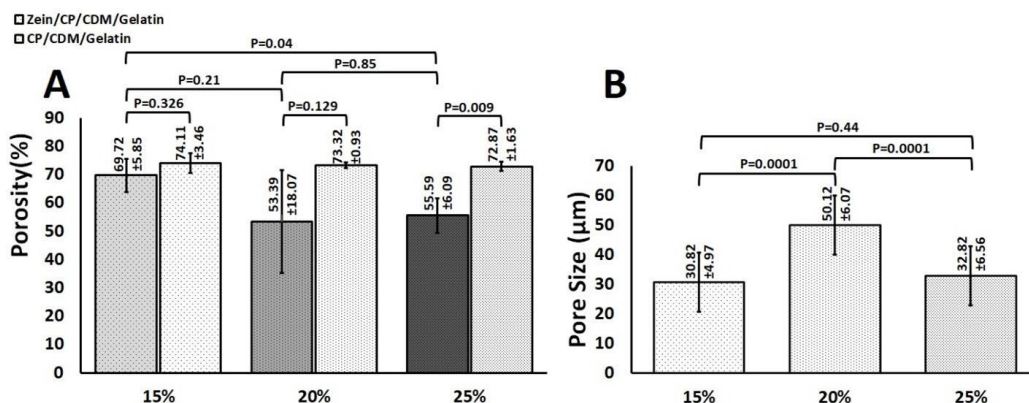


Figure 5. A) Comparison of the porosities between CDM/CP/gelatin and multi- phasic Zein/CP/CDM/gelatin scaffolds and B) Comparison between the pore sizes of multiphasic Zein/CP/CDM/gelatin scaffolds.

## Discussion

Various scaffolds have been explored in bone tissue engineering, yet they come with limitations, prompting the search for scaffolds with suitable structure, design and biocompatibility. Zein shows promise in bone regeneration due to its biocompatibility and mechanical attributes. Studies by Raucci MG, et al [25] and Zugravu MV, et al [26] highlighted the mechanical properties of different scaffolds, with our scaffold exhibiting a notable Young's modulus of 3.26 megapascals (Figure 8). This suggests the potential for modifying scaffold design to enhance mechanical strength. The study compared zein/Cp/collagen/Cp/gelatin nanofibers with a Control group, aiming to mimic bone's linear forces. Zein nanofibers were arranged in concentric circles to emulate bone's linear forces, enhancing the scaffold's ability to withstand pressure. This innovative design approach demonstrates the potential for developing scaffolds that mimic natural bone tissue, advancing bone tissue engineering.

The design of the zein/CP/collagen/CP/gelatin scaffold, as depicted in (Figure 9), effectively generated linear forces within the structure. Two groups were examined to confirm this: the first group included the scaffold with rolled zein nanofibers, while the control group lacked nanofibers containing calcium phosphate within collagen. Our research illustrates that the design with concentric circles leads to improved compressive strength and a 2.5-fold increase in Young's modulus.

Dynamic behavior tests were conducted to assess viscoelastic properties, typically involving 5 to 6 initial cycles for preconditioning loading. However, observations indicate variations in hysteresis behavior from the 6<sup>th</sup> to the 20<sup>th</sup> cycle. Comparison between Zein/CP/collagen/CP/gelatin scaffold and bone showed properties similar to trabecular bone. (Figure 10) shows the comparable compressive strength between the scaffold and the trabecular bone. Also as indicated in (Figure 11), the trabecular bone had approximately 76% porosity while the scaffold had approximately 56%. Nevertheless, this similarity emphasizes the potential of the scaffold, with opportunities for further modification to tune the porosity.

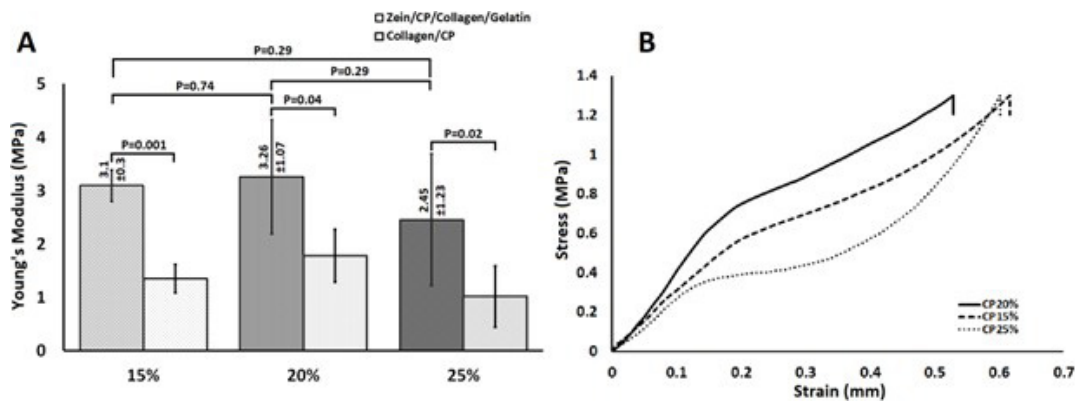


**Figure 6. A)** The Young's moduli of multiphasic Zein/CDM/CP/gelatin composite scaffolds and porous CDM/CP/gelatin controls with three different CP concentrations (15%, 20% and 25%) and **B)** The representative stress/strain curves for multiphasic Zein/CDM/CP/gelatin composite scaffolds with three different CP concentrations (15%, 20% and 25%).

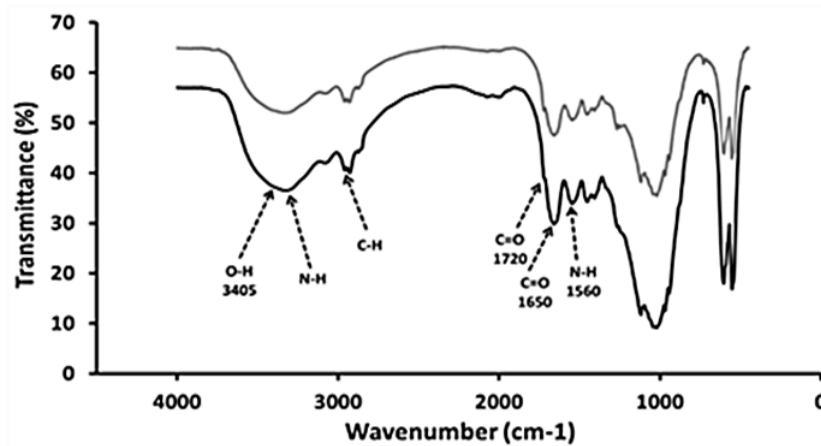


**Figure 7.** The FTIR spectra of Zein/CDM/CP/gelatin and Zein/CP.

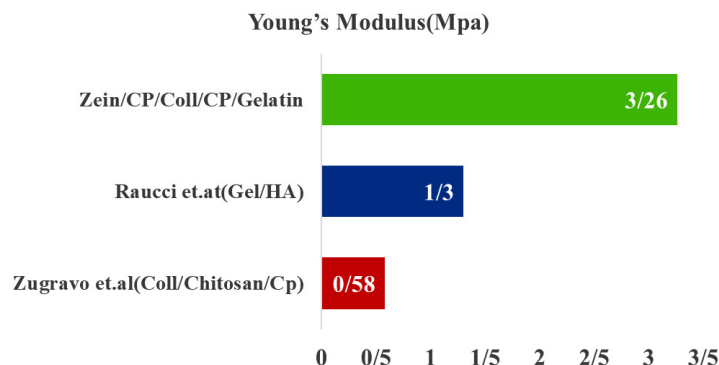


**Figure 8.** Comparison of mechanical characteristics between two almost similar scaffolds in previous studies with the scaffold made in this study.

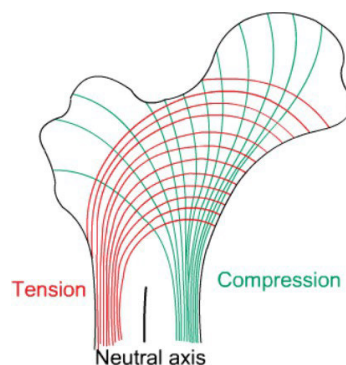


Figure 9. Stress line (Diagram showing computed lines of constant stress from the analysis of various transverse sections) [7].

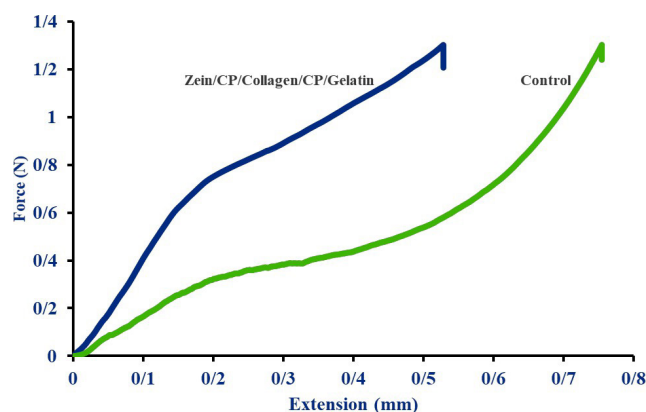


Figure 10. Comparison the mechanical properties of zein/CP/collagen/CP/gelatin scaffold and control.

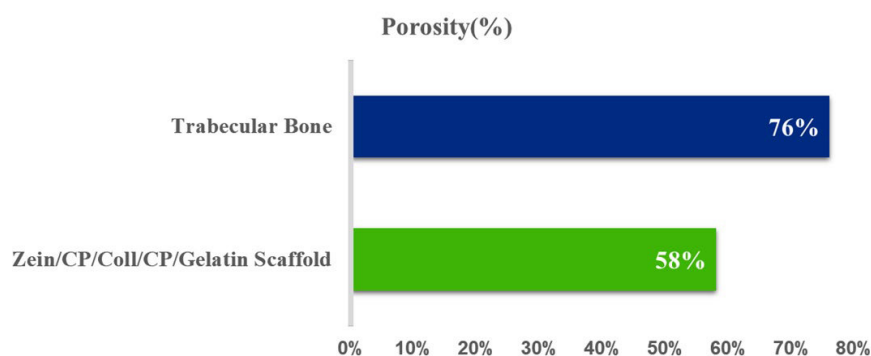


Figure 11. Comparison the porosity between zein/CP/collagen/CP/gelatin scaffold and control.

## Conclusion

A comparison of three concentrations of calcium phosphate (CP) in zein nanofibers 15%, 20% and 25% showed that the scaffold with 20% CP exhibited superior mechanical strength. Notably, in comparing 15% and 20%, the control group being zein/CP/collagen/CP/gelatin, the 15% concentration performed significantly better ( $P < 0.01$ ). However, for the highest Young's modulus and strength, the 20% concentration proved superior. SEM analysis revealed that scaffolds with 20% CP had larger pore sizes, suggesting better cell growth and nutrition.

## Acknowledgement

None.

## Conflict of Interest

The authors declare no conflicts of interest.

## References

1. Polo-Corrales, Liliana, Magda Latorre-Estevés and Jaime E. Ramírez-Vick. "Scaffold design for bone regeneration." *J Nanosci Nanotechnol* 14 (2014): 15-56.
2. Ghassemi, Toktam, Azadeh Shahroodi, Mohammad H. Ebrahimzadeh and Alireza Mousavian, et al. "Current concepts in scaffolding for bone tissue engineering." *Arch Bone Jt Surg* 6 (2018): 90.
3. Mastrogiacomo, Maddalena, Anita Muraglia, Vladimir Komlev and Francoise Peyrin, et al. "Tissue engineering of bone: Search for a better scaffold." *Orthod Craniofac Res* 8 (2005): 277-284.
4. Abdelaziz, Ahmed G, Hassan Nageh, Sara M. Abdo and Mohga S. Abdalla, et al. "A review of 3D polymeric scaffolds for bone tissue engineering: Principles, fabrication techniques, immunomodulatory roles and challenges." *Bioengineering* 10 (2023): 204.
5. Janmohammadi, Mahsa, Zahra Nazemi, Amin Orash Mahmoud Salehi and Amir Seyfoori, et al. "Cellulose-based composite scaffolds for bone tissue engineering and localized drug delivery." *Bioact Mater* 20 (2023): 137-163.
6. Alonzo, Matthew, Fabian Alvarez Primo, Shweta Anil Kumar and Joel A, et al. "Bone tissue engineering techniques, advances and scaffolds for treatment of bone defects." *Curr Opin Biomed Eng* 17 (2021): 100248.



7. Singh, Narpinder, Sandeep Singh, Amritpal Kaur and Mandeep Singh Bakshi. "Zein: Structure, production, film properties and applications." (2012).
8. Sun, Cuixia, Lei Dai, Xiaoye He and Fuguo Liu, et al. "Effect of heat treatment on physical, structural, thermal and morphological characteristics of zein in ethanol-water solution." *Food Hydrocoll* 58 (2016): 11-19.
9. Lai, Huey-Min and Graciela W. Padua. "Properties and microstructure of plasticized zein films." *Cereal Chemistry* 74 (1997): 771-775.
10. Kasaa, Mohammad Reza. "Zein and zein-based nano-materials for food and nutrition applications: A review." *Trends Food Sci Tech* 79 (2018): 184-197.
11. Aytac, Zeynep, Runze Huang, Nachiket Vaze and Tao Xu, et al. "Development of biodegradable and antimicrobial electrospun zein fibers for food packaging." *ACS Sustain Chem Eng* 8 (2020): 15354-15365.
12. Ansarifard, Elham and Farid Moradinezhad. "Encapsulation of thyme essential oil using electrospun zein fiber for strawberry preservation." *Chem Biol Technol Agric* 9 (2022): 1-11.
13. Luraghi, Andrea, Francesco Peri and Lorenzo Moroni. "Electrospinning for drug delivery applications: A review." *J Control Release* 334 (2021): 463-484.
14. Anton, Formhals. "Method and apparatus for spinning." (1944).
15. Bombin, Adrian D. Juncos, Nicholas J. Dunne and Helen O. McCarthy. "Electrospinning of natural polymers for the production of nanofibres for wound healing applications." *Mater Sci Eng C* 114 (2020): 110994.
16. Gauthier, Rémy. "Crack propagation mechanisms in human cortical bone on different paired anatomical locations: biomechanical, tomographic and biochemical approaches." (2017).
17. Rahmati, Maryam, David K. Mills, Aleksandra M. Urbanska and Mohammad Reza Saeb, et al. "Electrospinning for tissue engineering applications." *Prog Mater Sci* 117 (2021): 100721.
18. Thompson, C.J., George G. Chase, A.L. Yarin and D.H. Reneker. "Effects of parameters on nanofiber diameter determined from electrospinning model." *Polymer* 48 (2007): 6913-6922.
19. Massaro, Maria Stefania, Richard Palek, Jachym Rosendorf and Lenka Červenková, et al. "Decellularized xenogeneic scaffolds in transplantation and tissue engineering: Immunogenicity vs. positive cell stimulation." *Mater Sci Eng C* 127 (2021): 112203.
20. Yari, Davood, Jebrael Movaffagh, Mohammad Hosein Ebrahimzadeh and Arezoo Saberi, et al. "Biomimetic ECM-based hybrid scaffold for cartilage tissue engineering applications." *J Polym Environ* (2024): 1-19.
21. Moradi, Ali. Development of bovine cartilage extracellular matrix as a potential scaffold for chondrogenic induction of human dermal fibroblasts.
22. Moradi, Ali, Sumit Pramanik, Forough Ataollahi and Tunku Kamarul, et al. "Archimedes revisited: Computer assisted micro-volumetric modification of the liquid displacement method for porosity measurement of highly porous light materials." *Anal Methods* 6 (2014): 4396-4401.
23. Uskoković, Vuk and Dragan P. Uskoković. "Nanosized hydroxyapatite and other calcium phosphates: Chemistry of formation and application as drug and gene delivery agents." *J Biomed Mater Res B* 96 (2011): 152-191.
24. Schopper, Christian, Farzad Ziya-Ghazvini, Walter Goriwoda and Doris Moser, et al. "HA/TCP compounding of a porous CaP biomaterial improves bone formation and scaffold degradation-A long-term histological study." *J Biomed Mater Res* 74 (2005): 458-467.
25. Raucci, Maria Grazia, Christian Demitri, Alessandra Soriente and Ines Fasolino, et al. "Gelatin/nano-hydroxyapatite hydrogel scaffold prepared by sol-gel technology as filler to repair bone defects." *J Biomed Mater Res* 106 (2018): 2007-2019.
26. Zugravu, Monica V., Richard A. Smith, Benjamin T. Reves and Jessica A. Jennings, et al. "Physical properties and *in vitro* evaluation of collagen-chitosan-calcium phosphate microparticle-based scaffolds for bone tissue regeneration." *J Biomater Appl* 28 (2013): 566-579.

**How to cite this article:** Shahroodi, Azadeh, Sogol Hooshyar, Davood Yari and Jebrael Movaffagh, et al. "Fabrication, Characterization and Optimization of Multiphasic Zein/Cartilage-derived Matrix/CP/Gelatin Composite Scaffolds for Potential Bone Tissue Engineering Applications." *J Tiss Sci Eng* 15 (2024): 351.